DOI: 10.1021/ma100621f

Macromolecules
ARTICLE

Island Nucleation and Growth Dynamics during Submonolayer Vapor Deposition Polymerization

I.J. Lee* and Mira Yun

Department of Physics, Research Institute of Physics and Chemistry, Chonbuk National University, Jeonju, 561-756, Republic of Korea

Received March 22, 2010; Revised Manuscript Received May 4, 2010

ABSTRACT: The evolution of island formation during submonolayer growth of poly(chloro-*p*-xylylene) films on naturally grown silicon oxide substrates is investigated using atomic force microscopy (AFM), and analyzed within the framework of dynamic scaling theory. A transition of film growth mechanism from diffusion-limited aggregation to reaction-limited aggregation is dramatically displayed in an unprecedented progression of the island density distribution functions. As surface coverage increases, a conventional bell-shaped monomodal distribution in early growth regime ($\theta = 0.07$) gradually changes to a monotonically decreasing function, approximately following a power-law. The marginal power-law scaling behavior of the island distribution functions, reminiscent of the behavior of colloid aggregation, strongly suggests that film growth by vapor deposition polymerization is a new type of surface growth governed by reaction-limited aggregation process in which the competition between diffusion and deposition does not define the typical time scale of film growth.

Introduction

Fundamental understanding of the growth of organic films, including the formation of islands and its temporal evolution, is currently a topic of substantial interest in an effort to fabricate high performance organic electronic devices.[1,2] The basic growth process of organic molecular semiconductors which involves formation of islands and its temporal evolution has been relatively well characterized and found to closely follow the conventional atomistic growth theory[3,4] developed to understand inorganic thin film growth by molecular beam epitaxy (MBE). According to previous studies of submonolayer growth of pentacene ($C_{22}H_{14}$) films,[5,6] the dendritic growth of islands on a silicon surface and the evolution of island size distribution with coverage have been well understood within conventional dynamic scaling theory[7,8] based on the diffusion-limited aggregation (DLA) model.[9,10] However, very little quantitative information exists about the initial stage of polymer film growth. During film growth by vapor deposition polymerization, the biradical nature of monomer molecules[11] likely plays an interesting role and may lead to distinctive growth behaviors that are drastically different from what we would expect from the conventional atomistic film growth.

Plausible processes that may occur during vapor deposition polymerization are depicted in Figure 1. Monomer molecules were adsorbed on a substrate (a). The adsorbed monomer subsequently diffused (b) and the initiation reaction took place when two or more monomer molecules joined to form a biradical oligomer (c). The propagation reaction occurred when a monomer molecule encountered one of the free-radical polymer chain-ends (d). It is generally known that the rate of consumption of monomers by the propagation is several orders of magnitude greater than the consumption rate by the initiation at room temperature.[11] The size of the island (or cluster of polymer chains) grew in both the lateral and vertical directions with the help of the propagation reaction and the aromatic interactions which function practically as a diffusion bias for the upper layer growth. The aromatic $\pi-\pi$ interactions between the surface of flat aromatic rings made long polymer chains entangle one another in such a way as to rearrange themselves like a stack of coins,[12,13] and thus the relaxations driven by the strong interchain interaction reconstruct the island more compact (f). As the result of relaxations, a partial screening of interaction energy between incoming monomers and active chain-ends may occur and make it difficult for monomers to complete propagation reaction on the first encounter. The island lost pairs of active ends whenever two

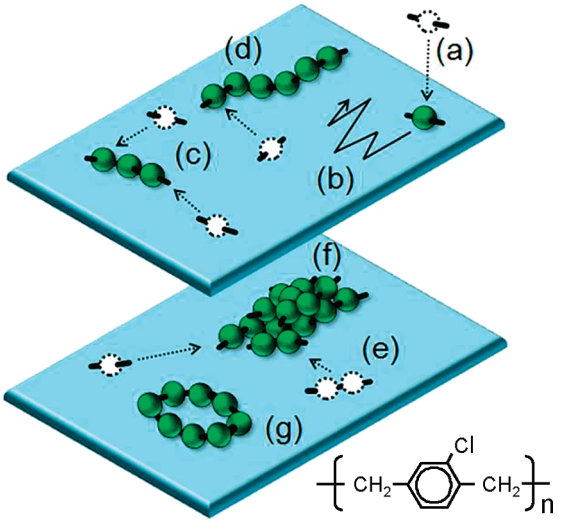

Figure 1. Conceivable processes during polymerization: (a) monomer deposition, (b) surface diffusion, (c) nucleation of the polymer chain or initiation reaction, (d) propagation reaction, (e) dimer diffusion, (f) entanglement of polymer chains due to intermolecular interactions, and (g) loop formation. The chemical structure of PPX-C is shown in the bottom of the right corner.

*Corresponding author: ijlee@chonbuk.ac.kr.

 Published on Web 05/13/2010

independent polymer chain-ends were joined and formed a closed loop (g).

In their Monte Carlo study, Zhao et al.[14] considered the polymerization processes a−d depicted in Figure 1 and identified three characteristic growth regimes: a low coverage initiation regime, a chain propagation regime, and a saturation regime. They found that the scaling behaviors of island size, island density, and the island density distribution functions were essentially comparable with the results of the standard atomistic submonolayer growth theory[7,8] until surface coverage reaches the saturation regime at which island density diverges due to restrictions imposed on monomer−polymer chain and chain−chain interactions. Unfortunately, any peculiar growth characteristic which we can directly associate with polymerization process including the presence of the unusual saturation regime has not been confirmed. In this report, we present systematic studies of the evolution of island formation during the submonolayer growth of poly(chloro-*p*-xylylene) (PPX-C) films on naturally grown silicon oxide substrates. Interestingly, the outcome of dynamic scaling analysis strongly indicate that film growth by vapor-deposition polymerization belongs to a new type of surface growth governed by reaction-limited aggregation process in which the usual competition between diffusion and deposition does not define the typical time scale of film growth.

Experimental Methods

PPX-C films were synthesized in a custom built chemical vapor deposition reactor consisting of a sublimation furnace, a pyrolysis furnace, and a deposition chamber backed by a diffusion pump. Dimer molecules (dichloro-di-*p*-xylylene) of granular type were sublimed at 120 °C and then cracked into monomers in the pyrolysis furnace at 660 °C. The monomers were subsequently condensed and polymerized on SiO_2/Si substrates in the deposition chamber, which is held at room temperature. Several atomically clean substrates having a typical rms roughness of 0.15 nm were arranged on a substrate holder which was equipped with a grease-sealed shutter to prevent impurities and volatile contaminants of the dimer molecules from condensing on the substrates during the evacuation of the entire deposition system and during the initial warming-up of the sublimation chamber. We found that the use of a substrate shutter was crucial to study genuine properties of the initial stage of island formation without secondary effects which were associated with contaminants condensed on the substrate during the deposition system reached an equilibrium condition. After several atomically clean SiO_2/Si substrates were exposed to the monomer flux for a fixed duration, the samples were taken out of the chamber and the surface morphology was measured using AFM (XE-100, Park systems) in a noncontact mode with various scan sizes in the range of 0.5 × 0.5 to 3 × 3 μm^2. When the film was partially covered, the film thickness was determined by averaging the mean-height values from the histograms of several AFM images taken from each film after the contributions from the bare substrate had been subtracted.[15] During the submonolayer PPX-C film growth, a growth rate of 1−2 nm/min was maintained.

Results and Discussion

Evolution of AFM images of islands projected onto the substrate in submonolayer regime of the PPX-C films is presented in Figure 2. The thicknesses d = 0.17, 0.47, 1.56, 2.93, 5.65, and 10.7 nm correspond to the surface coverage θ = 0.07, 0.21, 0.41, 0.48, 0.70, and 0.87, respectively. Each image was taken with 512 by 512 pixels so that the least discernible island in terms of a pixel corresponds to approximately 3 monomer-lengths in size. Strong intermolecular interactions between polymer chains produce compact islands with smooth edges in the growth stage as early as θ = 0.07 (see also the inset of Figure 5). Until islands coalesce

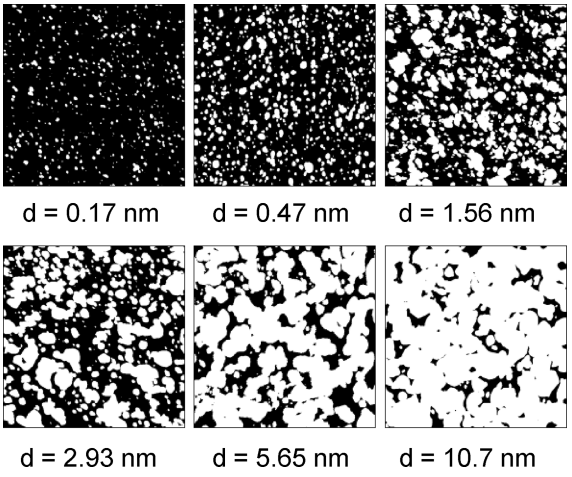

Figure 2. Representative two-dimensional AFM images (1 μm × 1 μm) of islands in submonolayer regime of the PPX-C films.

at $d \sim 1$ nm, the average aspect ratio (i.e., ratio of the lateral to the vertical size of an individual island) was measured well below 10^{-1}, maintaining more or less two-dimensional growth. At d = 1.56 nm, island coalescence is evident as indicated by asymmetric shape of islands dominating the entire scan area. A percolation at which the lateral size of an island spans the system size is also noticeable at d = 5.65 nm. With facilitated diffusion of monomers on the substrate, we expect the complex polymerization process to exhibit interesting growth characteristics that are quite different from those of the usual epitaxial film growth. To obtain insight into the mechanism governing the lateral growth of island due to propagation reaction, we employ two-dimensional dynamic scaling analysis which has been practically used to investigate various forms of islands ranging from one-dimensional metal rows to three-dimensional droplet patterns.[16−18]

The temporal evolution of island (or cluster of polymer chains) density (a) mean island size taken as a side of an equivalent square area (b), obtained from PPX-C films in the submonolayer growth regime, is shown in Figure 3. The inset of panel a displays the surface coverage as a function of film thickness. The island density was given as the number of islands divided by total available sites. The site area was estimated approximately 0.42 nm^2 under the assumption that the aromatic rings in PPX-C film were oriented parallel to the substrate.[12,13] Interestingly, the saturation regime identified by a substantial increase in N due to drastic increase of small islands, which was predicted in the previous simulation study involving processes a−d of Figure 1, was not observed. Rather, the temporal evolution of N and L appear to closely follow the conventional atomistic model displaying characteristic regimes of submonolayer epitaxial film growth:[3,7] the intermediate coverage regime at which N grows with a power-law, the aggregation scaling regime where N remains a constant,[19] and the coalescence/percolation regime where N decreases. In addition, as displayed in the inset of Figure 3a, the surface coverage grows proportional to the film thickness. While the observations of conventional scaling behaviors are rather surprising given that the island formation by polymerization involves processes very different from those associated with the usual inorganic film growth such as MBE, they provide us reasonable grounds for applying every aspect of the conventional dynamic scaling theory to the polymer system.

However, the substantial slowing down of the growth rate of the surface coverage $\theta(d)$ in the coalescence regime, which amounts to one tenth of the initial growth rate, is hard to make sense within simple conventional growth models even with taking a possible overlayer growth into account. It is important to note

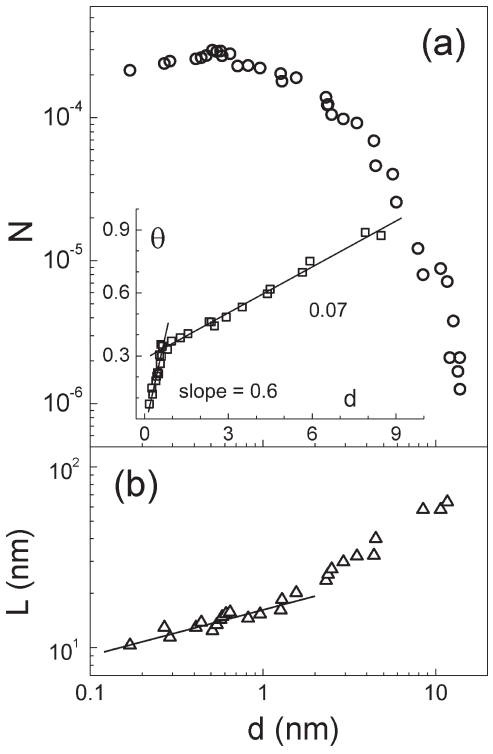

Figure 3. A log−log plot of (a) island density N and (b) linearized mean island size L as a function of average film thickness. The inset displays surface coverage versus film thickness. The slope of the linear best fit is shown as a line in each panel.

that the parameters at the crossover ($\theta \sim 0.35$, $d \sim 0.68$ nm) closely match the point where the coalescence regime begins, as clearly signaled by the reduction of N and the enhancement in the growth rate of mean island size L occurring for $d \geq 1$ nm. The number of monomers adsorbed on top of an existing island and held there by aromatic interactions is likely proportional to the mean island size (L). Therefore, the 2-fold increase in the growth rate of L for $d \geq 1$ nm naturally takes part in the slowing down of $\theta(d)$, but it certainly fall short of being a full account for the substantial reduction as seen. Since the lateral growth of islands occurs through the propagation reaction depicted as part d in Figure 1, it seems reasonable to attribute the substantial slowing down of $\theta(d)$ to the processes f and g. In fact, during island coalescence, a significant portion of free radical chain-ends in the outskirt of merging islands overlaps and becomes hidden from the reach of impinging monomers as a result of complicated postdeposition relaxations. When the system is deprived of the major means of lateral growth, i.e., the propagation reaction, the growth rate of coverage should be reduced. Furthermore, since there are many encounters before a monomer bonds to one of the radical chain-ends, the lateral growth of island through successful propagation reaction should be retarded. This slow aggregation process is limited not by diffusion but by the strength of the chemical reactivity, which is a characteristic growth property frequently found in colloidal aggregation and known by the so-called reaction-limited aggregation (RLA).[20,21]

Now, we consider the size distribution of islands, which should reveal details of the prevailing aggregation mechanism. According to the conventional dynamic scaling theory of film growth, the onset of the aggregation scaling regime is signaled by a plateau of the island density before system enters the coalescence regime. When mean island size R is only one characteristic length scale in the system, the distribution of island sizes s at a coverage θ, $N_s(\theta)$, takes the general scaling form[4,7] $N_s(\theta) = \theta R^{-2} f(u)$ where $u = s/R$ and $f(u)$ is a dimensionless scaling function. Exclusively

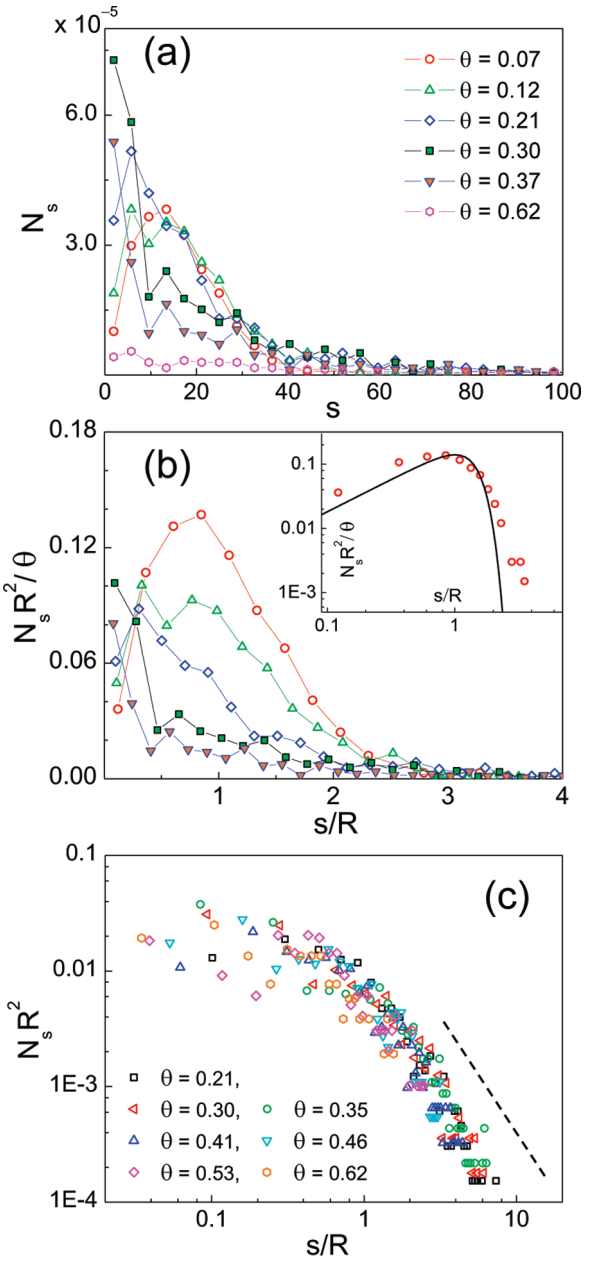

Figure 4. (a) Polymer island (or chain) densities as a function of polymer chain length for various surface coverage. (b) Scaled island distribution functions. The inset shows a log−log plot of the distribution function measured (symbols) and calculated (solid line) at $\theta = 0.07$. (c) A log−log plot of the function $f \equiv N_s R^2$ versus s/R for various θ. The dotted line of a slope of −2 is a guide for the eyes.

on the basis of Figure 3, we find that the surface coverage in the ranges of $0.2 < \theta < 0.35$ (or 0.45 nm $< d <$ 0.68 nm) belongs to the aggregation scaling regime in which the scaled distribution functions collapse to a single bell-shaped curve.

Figure 4a shows the island density distribution functions at various values of surface coverage. The mean island size R and the individual island size s were taken as a side of an equivalent square area of the corresponding islands in terms of the monomer length (0.65 nm) which we took as naïve estimate of a nominal chain length constituting an island. The progression and the shape of the distribution functions with coverage is in stark contrast with what the conventional atomistic growth theory predicts.[4,7] The gradual change in the shape of distribution function, from monomodal to monotonically decreasing form, strongly suggests that there has been a significant modification in

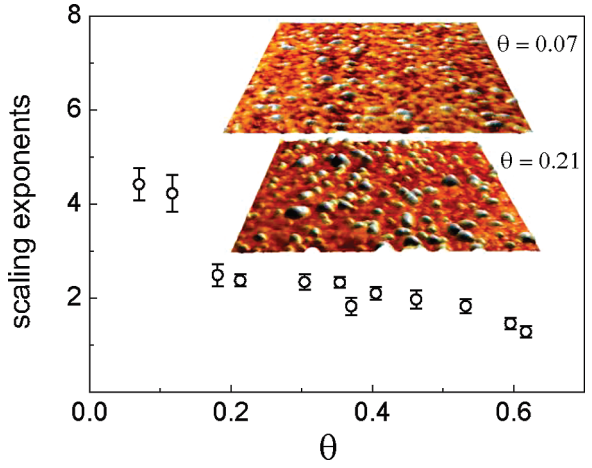

Figure 5. Variation of the power-law scaling exponents as a function of surface coverage. The inset shows a perspective view of AFM images taken at $\theta = 0.07$ and 0.21 with a scan size of 500 × 500 nm^2. The vertical scale of each image is magnified by a factor of 3 for clear view.

aggregation mechanism. The peak of the monomodal distribution at $\theta = 0.07$ is shifted toward smaller s values and then disappears as coverage increases. One of apparent reasons for the unusual evolution can be attributed to the accumulation of small islands. It is worthy of noticing that the value of N_s for small s increased until $\theta \sim 0.3$, and then decreased as the system underwent the coalescence regime. This extraordinary evolution of small islands is probably associated with the complicated screening action of chemical reactivity which is dramatically manifested as the substantial reduction of $\theta(d)$ in the coalescence regime (see the inset of Figure 3a). When polymer chains within a small island lose pairs of active ends (e.g., via the processes f and g in Figure 1) and become inactive, the lateral growth of the island by propagation reaction will be stopped or significantly hampered. Naturally, a number of small inactive islands accumulate with coverage until they are consumed by other active islands in the coalescence regime. We note that, in recently proposed kinetic model for free-radical polymerization processes,[22] the size distribution of inactive polymer chains was found to depend strongly on the details of reaction-rate kernels.

A substantial modification of the scaling function due to strong chemical reactivity is clearly seen in the scaling plot Figure 4b. As coverage increased, a bell-shaped monomodal island distribution at $\theta = 0.07$, a characteristic growth by DLA, gradually disappeared and became a monotonically decreasing function with extended tails approximately following a power-law. In the intermediate coverage regime, the scaled distribution function at $\theta = 0.07$ as shown in the inset of Figure 4b was found to follow closely the solid line which was obtained from an empirical distribution function[6,23] for a stable island size of two monomers. In the aggregation scaling regime, the outlines of scaling function between $\theta = 0.2$ and 0.37 are expected to collapse to single monomodal curve[24] as long as conventional DLA works regardless of the individual patterns of islands[17,18] or the difference in chemistry involved in submonolayer growth.[20,25] Note that the shape of scaling curves between $\theta = 0.2$ and 0.37 are clearly in transit from monomodal to monotonically decreasing function. It is clear that the expected data collapse to single monomodal curve is not possible no matter what the scaling scheme we choose, whether we use either the linearlized size or the island area as usual for the conventional scaling plot. Moreover, as we further discuss regarding the scaling of distribution functions, the current scaling scheme using the nominal chain length may seem plausible in its own right. The clear absence of data collapse to single monomodal curve and most of all the unexpected evolution discovered in the density distribution function strongly indicate that there has been a drastic change in the growth mechanism due to strong chemical reactivity involved in the polymerization process. It is important to note that this rare progression of the scaled distribution function occurs prior to the coalescence regime ($\theta \leq 0.37$) in which the scaling properties of growth parameters (see Figure 3) are still pointing that conventional atomistic growth is in operation. Interestingly, as shown in Figure 4c, data of $\theta \geq 0.2$ show marginal scaling behavior for $s/R \geq 1$ with a slightly different scaling scheme, $N_s(\theta)R^2$, which is essentially the scaling function employed to describe the irreversible reaction-limited aggregation of colloidal systems.[20,21] Furthermore, as shown by the dotted line, the scaling exponent is obtained close to −2, which is not far from that of the colloid-like RLA in which an exponent of −1.5 was reported.[20,21] Since the colloidal aggregation model does not allow addition of new particles via deposition, and a large cluster−cluster aggregation is not practical during polymerization as evidenced by the inset of Figure 4b, a strict application of the colloid model to the surface polymerization may have some limitations. One of the most noticeable differences is that in the polymerization process, the power-law scaling of the island density distribution exists not in the small island side ($s/R \leq 1$) but in the large island side ($s/R \geq 1$) where, instead of the power-law, an exponentially decaying function has been observed for the usual reaction-limited colloid aggregation. In any event, the characteristics of the power-law scaling provide us two important clues: one is that the RLA starts to affect the island distribution function in early stage of the polymer growth well before the coalescence regime begins, and the other is that the activation of the RLA is closely related to the size of island (or more accurately, average chain length constituting islands).

When islands are small and well separated such as in the case $\theta = 0.07$, active chain-ends are well exposed and may be evenly distributed along the edges of islands. For the most of diffusing monomers, it is easy to make a bond with chain-ends whenever they collide with the edges of islands. The time-averaged spatial distribution of adsorbed monomer density decays to zero at the edges of island, which is a condition for the monomodal distribution of island size as we know from conventional growth models. The spatial variation of monomer density near the edges of islands can be easily visualized with the capture zone model.[26] As island grows, so does the energy of interchain interaction due to increase in the number of aromatic rings constituting a polymer chain. At some point of the growth, the chain−chain interaction becomes strong enough to clump polymer chains in a stack (island), resulting in a partial screening of the interaction energy between impinging monomers and polymer chain-ends, and making it hard for monomers to bond on the first encounter. Perhaps in the presence of a number of adsorbed monomers wandering around the edges of island, the time-averaged spatial distribution of monomer density may become more or less uniform across the substrate, satisfying a basic condition for the Avrami model for grain growth[27] which is known to yield the island size distribution of power-law form.[28,29] A similar growth condition to the case of RLA may be reproduced if a finite probability of islands absorbing monomers is incorporated into conventional submonolayer growth model, which according to simulation studies[29] may exhibit monotonically decreasing island distribution functions.

Variation of the power-law scaling exponents as a function of surface coverage is shown in Figure 5. The tail section of the scaling function, N_sR^2 versus s/R, was fitted with a power-law function. The negative sign of the power-law exponents was dropped for the construction of Figure 5. The large error bars near $\theta = 0.1$ were due to the fact that a power-law function was forced to fit the island distribution in the low coverage regime

where an exponentially decaying tail was apparent. The transition coverage (θ_t) at which the aggregation mechanism crosses over from DLA to RLA should be placed near $\theta_t = 0.15$ corresponding to the sudden drop of the scaling exponent. The inset shows topological images taken before and after the transition surface coverage. Each individual island exhibits characteristics of amorphous growth without step edges and shows no particular change in structure other than its sizes as the surface coverage increases. Finally, when two-dimensional island area, instead of the linearized size representing a nominal chain length of an island, was used for the size distribution functions, the scaling exponents were reduced. In the RLA regime, the mean exponent was obtained around 1. Nevertheless, since the general dependence of scaling exponents on the surface coverage was maintained the same as Figure 5, the transition surface coverage was consistently determined at $\theta_t = 0.15$. In polymer film growth, each island can be treated as a stack of linear chains. If we consider the fact that the data at $\theta = 0.07$ follows closely an empirical function (see the inset of Figure 4b) and that a marginal scaling behavior persists in the wide range of coverage as displayed in Figure 4c, taking the nominal chain length as a characteristic length scale for the size of island does not seem too far-fetched.

Conclusions

The lateral growth of islands during submonolayer growth of PPX-C films on silicon oxide substrate is investigated using AFM and analyzed within the framework of dynamic scaling theory. The scaling properties of the growth parameters such as the evolution of island density ($N(d)$), surface coverage ($\theta(d)$), and mean island size ($L(d)$) appear to closely follow what we would expect from simple atomistic models for epitaxial film growth. Intrinsic properties of polymerization processes are most dramatically manifested in the evolution of island density distribution functions. From detailed scaling analysis, a transition surface coverage (θ_t) at which the shape of island distribution function changes from monomodal to monotonically decreasing form is identified. The unprecedented progression of the distribution functions through θ_t is interpreted as a crossover of aggregation mechanism from DLA to RLA. The marginal power-law scaling behavior, reminiscent of colloid aggregation, is found to persist deep in the coalescence regime. Since the lateral growth of islands is made through propagation reaction, it depends strongly on the energy of chemical reactivity at the radical chain-ends. Both peculiar phenomena, the unusual evolution of island distribution functions near the transition surface coverage and the substantial slowing down of the surface coverage at the coalescence regime, were consistently understood by considering some delicate modifications in the interaction energy occurring at the chain-ends (edges of island).

Island size distribution functions have been observed in the form of either conventional bell-shaped monomodal or monotonically decreasing functions. We believe that the submonolayer growth of polymer film is the first example displaying an interesting connection between two types of island distribution functions. We hope that the results and analysis can be extended to other similar organic systems where molecular interactions and relaxations are expected to play an important role.

Acknowledgment. We thank M. Ha for useful discussions. This work was supported by the Korea Science and Engineering Foundation Grant No. R01-2006-000-10800-0 and by Korea Research Foundation Grant No. KRF-2008-313-C00336.

References and Notes

(1) Someya, T.; Kato, Y.; Sekitani, T.; Iba, S.; Noguchi, Y.; Murase, Y.; Kawaguchi, H.; Sakurai, T. *Proc. Natl. Acad. Sci. U.S.A.* **2005**, *102*, 12321–12325.
(2) Kim, C.; Facchetti, A.; Marks, T. J. *Science* **2007**, *318*, 76–80.
(3) For comprehensive review, see: Evans, J. W.; Thiel, P. A.; Bartelt, M. C. *Surf. Sci. Rep.* **2006**, *61*, 1–128.
(4) Barabasi, A.-L.; Stanley, N. E. *Fractal Concepts in Surface Growth*; Cambridge University Press: Cambridge, U.K., 1995.
(5) Meyer zu Heringdorf, F.-J.; Reuter, M. C.; Tromp, R. M. *Nature* **2001**, *412*, 517–520.
(6) Ruiz, R.; Nickel, B.; Loch, N.; Feldman, L. C.; Hagulund, R. F.; Kahn, A.; Family, F.; Scoles, G. *Phys. Rev. Lett.* **2003**, *91*, 136102.
(7) Amar, J. G.; Family, F.; Lam, P.-M. *Phys. Rev. B* **1994**, *50*, 8781–8797.
(8) Jensen, P.; Barabasi, A.-L.; Larralde, H.; Havlin, S.; Stanley, H. E. *Phys. Rev. B* **1994**, *50*, 15316–15329.
(9) Witten, T. A.; Sander, L. M. *Phys. Rev. Lett.* **1981**, *47*, 1400–1403.
(10) Meakin, P. *Phys. Rev. A* **1983**, *27*, 1495–1507.
(11) Beach, W. F. *Macromolecules* **1978**, *11*, 72–76.
(12) Isoda, S.; Kawaguchi, A.; Katayama, K.-I. *J. Polym. Sci., Polym. Phys. Ed.* **1984**, *22*, 669–679.
(13) Park, S.-Y.; Blackwell, J.; Chvalun, S. N.; Nikolaev, A. A.; Mailyan, K. A.; Pebalk, A. V.; Kardash, I. E. *Polymer* **2000**, *41*, 2937–2945.
(14) Zhao, Y.-P.; Hopper, A. R.; Wang, G.-C.; Lu, T.-M. *Phys. Rev. E* **1999**, *60*, 4310–4318.
(15) Lee, I. J.; Yun, M.; Lee, S.-M.; Kim, J.-Y. *Phys. Rev. B* **2008**, *78*, 115427.
(16) Albao, M. A.; Evans, M. M. R.; Nogami, J.; Zorn, D.; Gordon, M. S.; Evans, J. W. *Phys. Rev. B* **2005**, *72*, 035426.
(17) Ebiko, Y.; Muto, S.; Suzuki, D.; Itoh, S.; Shiramine, K.; Haga, T. *Phys. Rev. Lett.* **1998**, *80*, 2650–2653.
(18) Brinkmann, M.; Biscarini, F.; Taliani, C.; Aiello, I.; Chedini, M. *Phys. Rev. B* **2000**, *61*, R16339–R16342.
(19) Under assumption that the system is governed by diffusion mediated growth, the value $G = D/F$, where D is the diffusion constant and F is the monomer flux, can be estimated from the peak island density which scales as $N_{max} \cong 0.43G^{-0.34}$ (ref 7) and independently from the analytical solution of the point island model which results in $N_{max} \cong (G\ lnG)^{-1/3}$. Using the measured value of $N_{max} = 2.9 \times 10^{-4}$ (Figure 3a), we obtain $G = 2.1 \times 10^9$ for the former and $G = 1.9 \times 10^9$ for the latter, respectively.
(20) Broide, M. L.; Cohen, R. J. *Phys. Rev. Lett.* **1990**, *64*, 2026–2029.
(21) Gonzalez, A. E. *Phys. Rev. Lett.* **1993**, *71*, 2248–2251.
(22) Yang, S.-Y.; Zhu, S.-O.; Ke, J. *Phys. Rev. B* **2009**, *80*, 031114.
(23) Amar, J. G.; Family, F. *Phys. Rev. Lett.* **1995**, *74*, 2066–2069.
(24) The scaling curves were constructed following the scheme of the theoretical study of vapor-deposition polymerization by Zhao et al.[14] The integral of the scaling function over all sizes was not normalized to unity. But, as long as R is only one characteristic length scale in the system, the integrals of each curve should produce a single finite value, which should allow us to do a uniform comparison of various curves in the particular scaling regime. In any event, it is important to notice that the unusual evolution of the scaled density distribution function remains the same independent of the details of scaling scheme.
(25) Doudevski, I.; Schwartz, D. K. *Phys. Rev. B* **1999**, *60*, 14–17.
(26) Mulheran, P. A.; Blackman, J. A. *Phys. Rev. B* **1996**, *53*, 10261–10267.
(27) Avrami, M. *J. Chem. Phys.* **1941**, *9*, 177–184.
(28) Mulheran, P. A.; Robbie, D. A. *Philos. Mag. Lett.* **1998**, *78*, 247–253.
(29) Robbie, D. A.; Mulheran, P. A. *Comput. Mater. Sci.* **2000**, *17*, 500–504.